The BaR-SPOrt Experiment

M. Zannoni[*], M. Baralis[†], G. Bernardi[**], G. Boella[*], S. Bonometto[*], A. Boscaleri[‡], E. Carretti[**], S. Cecchini[**], S. Cortiglioni[**], R. Fabbri[§], M. Gervasi[*], C. Macculi[**], J. Monari[¶], E. Morelli[**], V. Natale[‖], R. Nesti[††], L. Nicastro[‡‡], E. Pascale[‡], O. Peverini[†], S. Poppi[¶], C. Sbarra[**], G. Sironi[*], R. Tascone[†], M. Tucci[*] and G. Ventura[**]

[*] *Dip. di Fisica, Univ. di Milano - Bicocca, P.zza della Scienza 3, I–20126 Milano*
[†] *I.R.I.T.I./C.N.R., c.so Duca degli Abruzzi 24, I–10129 Torino*
[**] *I.Te.S.R.E./C.N.R., via P. Gobetti 101, I–40129 Bologna*
[‡] *I.R.O.E./C.N.R., Via Panciatichi 64, I–50127 Firenze*
[§] *Dip. di Fisica, Univ. di Firenze, Via Sansone 1, I–50019 Sesto Fiorentino, Firenze*
[¶] *I.R.A./C.N.R., via P. Gobetti 101, I–40129 Bologna*
[‖] *C.A.I.S.M.I./C.N.R., Largo E. Fermi 5, I–50125 Firenze*
[††] *Osservatorio Astrofisico di Arcetri, Largo E. Fermi 5, I–50125 Firenze*
[‡‡] *I.F.C.A.I./C.N.R., via U. La Malfa 153, I–90146 Palermo*

Abstract. BaR-SPOrt (Balloon-borne Radiometer for Sky Polarisation Observations) is an experiment to measure the linearly polarized emission of sky patches aboard a long duration stratospheric balloon. It consists of high sensitivity correlation polarimeters operating in the millimeter wavelength region and coupled to a telescope to obtain a sub-degree angular resolution for direct measurements of the Q and U Stokes parameters. This project shares most of the know-how and sophisticated technology developed for the SPOrt experiment aboard the International Space Station. The instrument design, the various solutions to reduce the systematics and the observing strategy are here described.

INTRODUCTION

The fine characteristics of Cosmic Microwave Background (CMB), spectral distortions, anisotropies and polarization, are the most sensitive tools to investigate the high red-shift Universe [1, 2, 3]. Since its discovery in 1965 [4], many efforts have been concentrated in a precise determination of the spectrum [5, 6, 7] and spatial distribution [8, 9, 10]. Current and near future space missions like MAP[1] and Planck[2] are mainly devoted to the all-sky mapping of CMB small-scale anisotropies for which they will reach the highest sensitivities. On the polarization side, against its unique capability to solve the degeneracy among cosmological parameters that anisotropy alone is not able to remove [2], only upper limits are available so far (see table 1), since either the foreseen polarized component of the CMB is definitely lower than the instrumental sensitivities or the contribution of the systematics dominates the final error budget. For these reasons dedicated experiments must be designed to attempt the CMB polarization detection. One of them will be the space mission SPOrt[3] which is described by Carretti et al. in this volume [11]. Direct spin-off of SPOrt is BaR-SPOrt, a balloon experiment funded by ASI (Italian Space Agency), which shares most of the know-how and technological development of the SPOrt program. Differently from SPOrt, the scientific goal of BaR-SPOrt is the mapping of the sky polarization of some low foreground regions with sub-degree angular resolution. In the following sections such a goal together with a review of the radiometer design and the observing strategies will be discussed in

[1] http://map.gsfc.nasa.gov/
[2] http://astro.estec.esa.nl/Planck/
[3] http://sport.tesre.bo.cnr.it/

more detail.

TABLE 1. Existing upper limits for the CMB linear polarization.

Resolution (deg)	Frequency (GHz)	Sky Coverage	Upper Limit	Reference
15	4	Scattered	300 mK	[4]
$1.5-40$	$100-600$	*GC*	3-03 mK	[12]
15	9.3	$\delta=+40°$	1.8 mK	[13]
15	33	$+37° \leq \delta \leq +63°$	180 μK	[14]
$18''-160''$	5	$\delta=+80°$	4.2 mK - 120 μK	[15]
1.2	$26-36$	*NCP*	30 μK	[16]
1.4	$26-36$	*NCP*	18μK	[17]
7	33	*SCP*	267 μK	[18]
$6'$	8.7	$\delta=-50°$	16 μK	[19]
0.24	90	*NCP*	13 μK	[20]
7	$26-36$	$\delta=+43°0$	10 μK	[21]

THE SCIENTIFIC MOTIVATION AND POSSIBLE TARGETS

Large scale CMB polarization (CMBP) measurements, due to the low level of the signal expected (see figure 1), need a very stable environment to be performed. For this reason all-sky surveys can be only carried out in space where very quiet and stable conditions exist. Ground-based and balloon-borne experiments can be devoted to small sky patches where they can reach sensitivities comparable with the expected level of polarization. As pointed out in [22], ground-based instruments operating in the millimeter domain are plagued by atmospheric emission which is the main source of spurious polarizations even in the best observing site like the Antarctic plateau. The instrumental polarization can correlate the unpolarized atmospheric signal, whose fluctuations can then degrade the expected sensitivity. The obvious consequence is to perform the observations from stratospheric altitude where the residual atmosphere and its contribution are negligible. Due to the limited observing time (a long duration flight can last about ten days - cfr [9]), typical targets are small ($\sim 20°x20°$) patches. On such portions of sky it is possible to study the sub-degree scales where the expected polarization peaks (see figure 1).

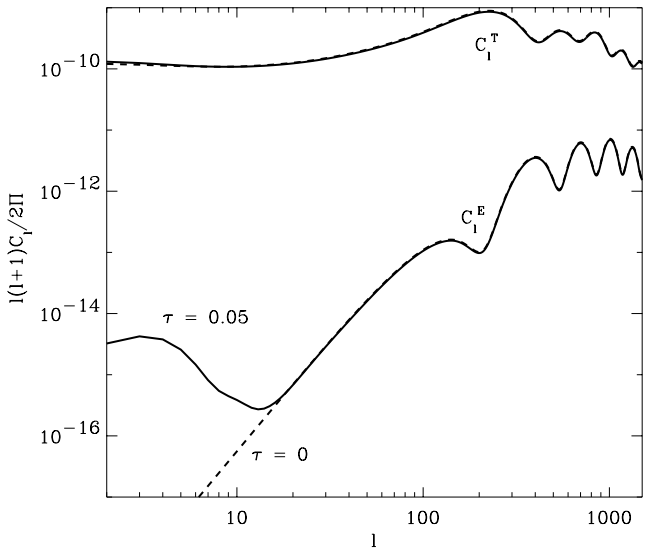

FIGURE 1. Anisotropy and E-mode power spectra. The expected polarized component of the CMB peaks in the sub-degree (high *l*) scales while the larger (degree) angular scales are more sensitive to the reionization scenarios.

Furthermore multifrequency deep scanning of small sky regions are also useful to understand how the polarized foregrounds contaminate a possible detection of CMBP. BaR-SPOrt is designed to carry on both these tasks.

Both in the Northern and in the Southern hemisphere sky patches of interest are available. The ideal regions, from the CMB point of view, are the ones at high galactic latitude, far from local cirrus, where the foreground should be minimal. In the Southern sky, the patch observed by BOOMERanG [9] ($\alpha = 5^h$, δ =-45°) is the ideal target, being opposite to the Sun during Summertime. Scaling from the Jonas map [23] at 2.3 GHz with a synchrotron spectral index $\gamma = 3$ ($T^{synch} \propto \nu^{-3}$) and with a ratio of $P^{synch}/T^{synch} = 0.1$, we can derive a level of polarization at 32 GHz (one of the channel of BaR-SPOrt) $\Delta P < 1\mu$K. The same thing can be done at 90 GHz starting from the DIRBE 240 μm map [24] and scaling the dust temperature as $T^{dust} \propto \nu^{2.7}/(e^{h\nu/kT_D} - 1)$ [25] with $P^{dust}/T^{dust} = 0.05$. The result is $\Delta P < 0.15\mu$K. For the region centered at ($\alpha = 10^h \delta = +35°$) in the Northern hemisphere, it is possible to derive, from the Reich [26] map at 1.4 GHz for the synchrotron contribution, $\Delta P < 0.3\mu$K @ 32 GHz and $\Delta P < 0.15\mu$K @ 90 GHz. In figure 2 the three maps [26, 23, 24] cited above have been scaled to 32 GHz and 90 GHz for the evaluation of synchrotron and dust contribution respectively; the selected patches in the Northern and Southern sky are shown in figure 2.

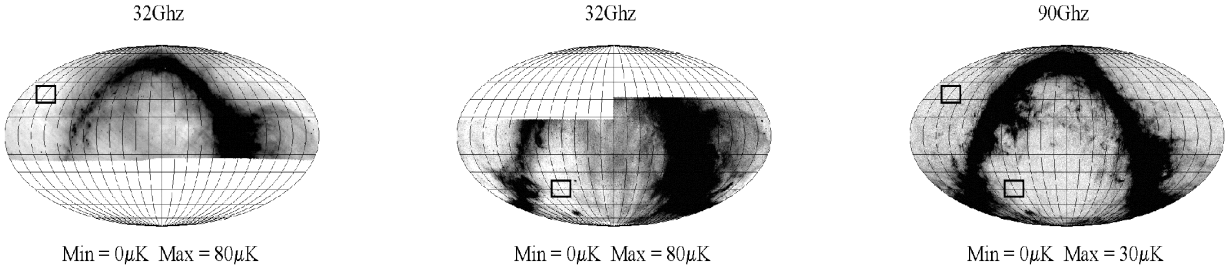

FIGURE 2. Foreground maps computed from the original public data in the radio [26, 23] and far infra-red [24] ranges. The first two have been rescaled to 32 GHz to evaluate the synchrotron component, while the last, related to the dust contribution, has been scaled down to 90 GHz. The two target patches have been superimposed.

From a logistical point of view, both patches are effectively observable. The one in the Southern Sky is accessible with a long duration balloon flight from the Mc Murdo Station in Antarctica, while the one in the Northern hemisphere can be observed during a flight launched from available facilities both in Norway [27] and in Sweden [28]. At the moment no final decision about the scanning strategies has been taken. Simulations are under development to optimize the patch dimension, scanning speed and path for maximizing the final full patch sensitivity. Expected raw sensitivities are reported in table 2.

TABLE 2. BaR-SPOrt expected sensitivities : σ_{1s} is the instantaneous sensitivity, σ_{PX} and σ_{FP} are the final per pixel and the full patch *rms* sensitivities for a flight of two weeks and a patch $20°x20°$ wide.

Frequencies (GHz)	**Bandwidth**	**Beamsize**	$\sigma_{1s}[\mathrm{mKs}^{1/2}]$	$\sigma_{PX}[\mu\mathrm{K}]$	$\sigma_{FP}[\mu\mathrm{K}]$
32	10%	0.5°	0.5	18	0.4
90	10%	0.2°	0.7	64	0.6

THE INSTRUMENT

The BaR-SPOrt payload houses correlation microwave polarimeters (32 & 90 GHz) for the direct measurement of the Q and U Stokes parameters with HPBW=0°.5 @32 GHz and 0°.2 @90 GHz (see figures 3 and 4). In the current baseline the two radiometers will be operated during different campaigns because only one feed at a time can be

housed on the optical axis of the telescope (at the moment we are oriented toward a Cassegrain scheme) to meet the very stringent requirements of extremely low spurious polarization (fractions of μK) necessary for such measurements (for a general discussion see [22]). The detection of signals as low as those expected from CMB polarisation (≤ 1 μK) implies the use of extremely sensitive and stable radiometers. BaR-SPOrt has been designed to minimize instrumental effects and to reduce $1/f$ noise, thereby increasing the long term stability. Great care has been taken in the realisation of the antenna system to control the spurious polarisation. Correlation techniques are widely adopted in high sensitivity measurements because of their capability to reduce the effects of gain fluctuations. Residual instabilities are recovered using destriping techniques [29, 30, 31, 32, 33], which require the radiometer to be stable only over a single scan period (the scanning time of BaR-SPOrt is between 30 and 60 seconds).

The main instrumental characteristics are:

- direct amplification architecture: no down conversion to avoid possible phase error;
- low cross-polarisation optics providing HPBW of $0^\circ.5$ ($0^\circ.2$) at 32 GHz (90 GHz);
- correlation unit based on a custom design waveguide Hybrid Phase Discriminator (HPD), with unpolarised component rejection $\geq$ 30 dB [34];
- custom design Orthomode Transducer (OMT) with high isolation between channels ($>$ 60 dB) to limit contaminations from the unpolarised component [32, 34];
- phase modulation (lock-in system) and correlation providing $>$ 70 dB of total rejection to the unpolarised component;
- a cryostat (see figures 5, 6) to cool to $T < (80.0 \pm 0.1)$ K the Low Noise Amplifiers, the circulators, the polariser and the OMT by a closed loop cryocooler. The horn, at present designed to be kept at $\approx$300 K, might be cooled as well. A thermal shield stabilised at temperature $T \cong (300.0 \pm 0.1)$ K, is foreseen to increase the thermal stability;
- custom design internal calibrator to inject reference polarised signals.

The block diagram of the radiometer is reported in figure 3.

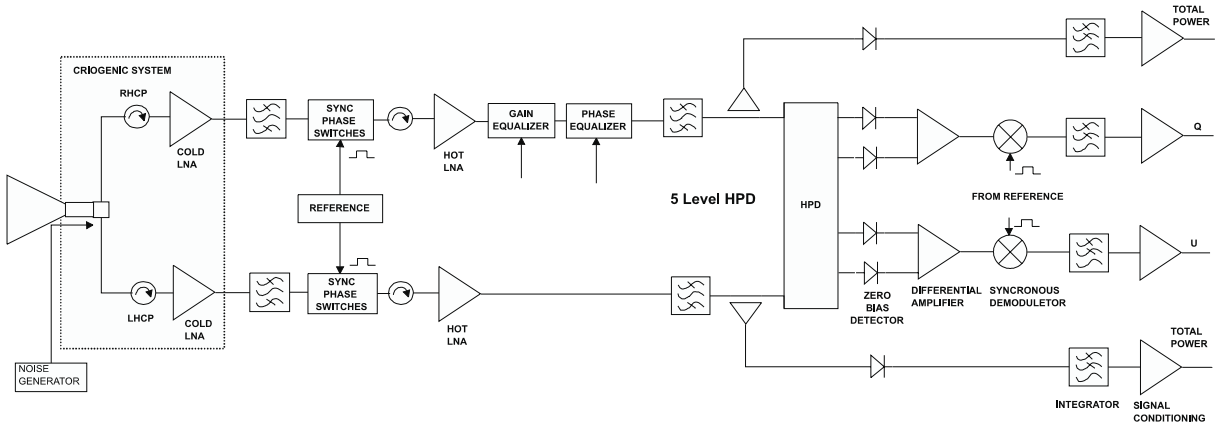

FIGURE 3. Block diagram of the BaR-SPOrt radiometers.

The antenna system collects the incoming radiation and transforms the linearly polarized components (E_x, E_y) of the electric field into the circularly ones (E_R, E_L) which are picked up by the Ortho-Mode Transducer (OMT) [35] (see figure 4).

A two positions ($0 - \pi$) phase shift after the first stage of amplification (LNA) provides phase modulation, followed by synchronous detection, in order to reduce the instability of the components inside the lock-in loop. Just before the Hybrid Phase Discriminator, a fraction of the signal is picked-up and fed into two total power detectors to record the Sky temperature and for monitoring of the System temperature too. The heart of the correlation unit is the HPD that processes the signal in order to have four outputs proportional to:

$$\vec{E_R} - \vec{E_L} \qquad \vec{E_R} + \vec{E_L} \qquad \vec{E_R} + j\vec{E_L} \qquad \vec{E_R} - j\vec{E_L} \tag{1}$$

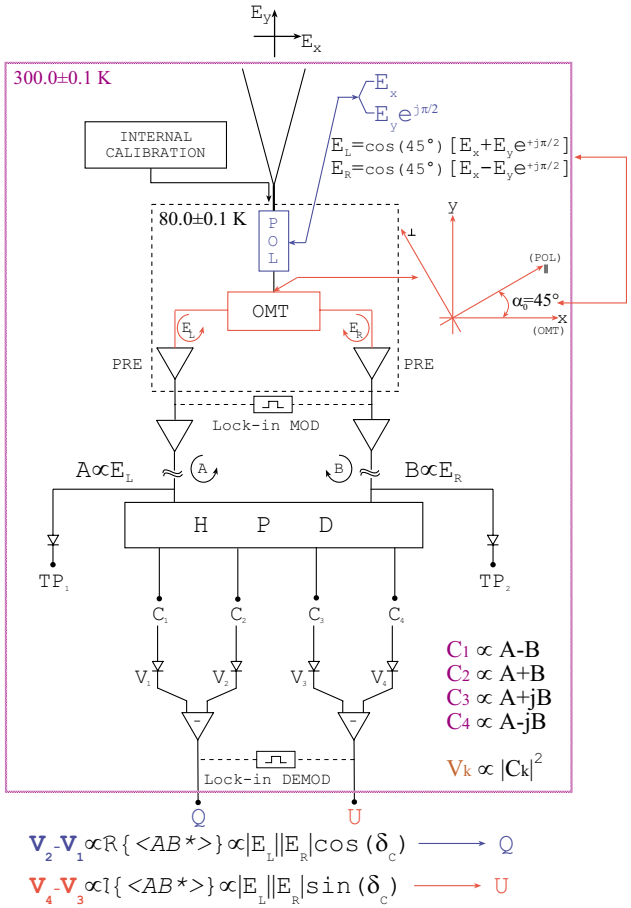

FIGURE 4. Scheme of the radiometers with the propagation of the fields collected by the feed horn.

After square law detection the four HPD outputs are:

$$\begin{aligned} V_1 &\propto [|\vec{E_L}|^2 + |\vec{E_R}|^2 - 2\Re(\vec{E_L}\cdot\vec{E_R}^*)] \\ V_2 &\propto [|\vec{E_L}|^2 + |\vec{E_R}|^2 + 2\Re(\vec{E_L}\cdot\vec{E_R}^*)] \\ V_3 &\propto [|\vec{E_L}|^2 + |\vec{E_R}|^2 + 2\Im(\vec{E_L}\cdot\vec{E_R}^*)] \\ V_4 &\propto [|\vec{E_L}|^2 + |\vec{E_R}|^2 - 2\Im(\vec{E_L}\cdot\vec{E_R}^*)] \end{aligned} \tag{2}$$

which are properly differentiated to get as final outputs the two quantities:

$$\begin{aligned} V_2 - V_1 &\propto |\vec{E_L}||\vec{E_R}|\cos(\delta_c) \longrightarrow Q \\ V_4 - V_3 &\propto |\vec{E_L}||\vec{E_R}|\sin(\delta_c) \longrightarrow U \end{aligned} \tag{3}$$

where δ_c is the phase delay between the two (L&R) circular components of the electric field. After integration, these provide time averaged values proportional to the Q and U Stokes parameters.

Since the BaR-SPOrt performances strongly depend on the temperature stability, particular care has been put in the thermal design. A mechanical Stirling cryocooler with closed loop control will provide the cooling down to 80 K with stability better than 0.1 K over the period of the flight (for some preliminary results on the performances of the cooler see [36]).

The vacuum needed for thermal isolation implies a large window in front of the feed which is housed inside the cryostat to keep stable its temperature (an active thermal control is also present in warm parts of the radiometer). Concerning the problem of the optical beam propagation through the window, great attention must be paid to the

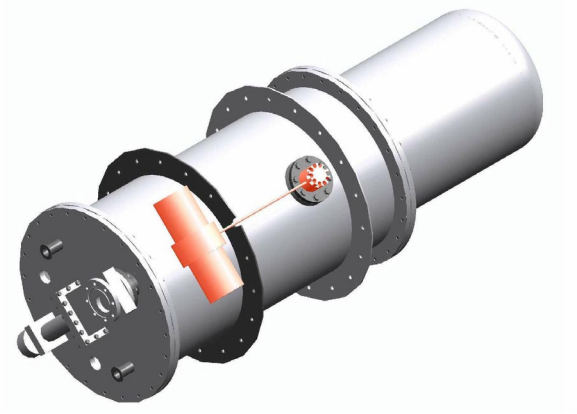

FIGURE 5. The cryostat housing the 32 GHz radiometer of BaR-Sport with the closed loop cryocooler visible in the foreground.

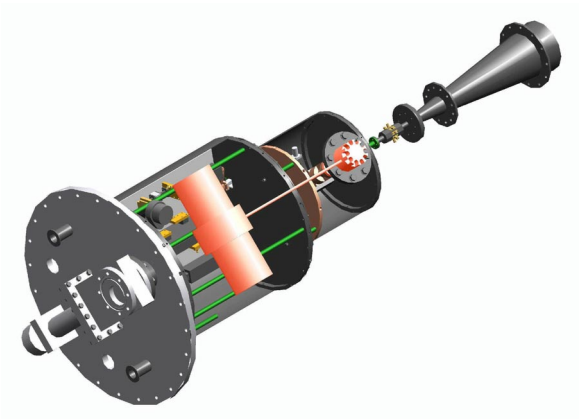

FIGURE 6. The radiometer inside the cryostat.

selection of the material of the vacuum window, even in the case of axial symmetry, which should ensure a null induced polarization. Some polymers have the necessary strength to sustain the pressure gap with very low internal stress [37], but show dichroism and birefringence [38]. This means that they are not suitable for polarization measurements. For many others materials there are no “optical” data in the microwave domain and our experimental team has started a parallel activity [39] to fully characterize a set of materials looking for the smallest spurious polarization.

CONCLUSIONS

The BaR-SPOrt experiment represents a good opportunity for testing in operative conditions state of the art technological solutions to be used in the incoming space mission SPOrt. It is also one of the first instruments with the potentiality to measure CMB polarization in small sky patches on sub-degree angular scale.

ACKNOWLEDGMENTS

Authors wish to thank the organizers of the Workshop for providing a great opportunity to show the BaR-SPOrt experiment. This work is partially supported by ASI.

REFERENCES

1. Jungman, G., Kamionkowski, M., Kosowsky, A., & Spergel, D. N. *PhysRevD*, 54, 1332-1344, 1996.
2. Zaldarriaga, M., Spergel, D. N., & Seljak, U. *ApJ* , 488, 1, 1997.
3. Efstathiou, G. & Bond, J. R. *MNRAS*, 304, 75, 1999.
4. Penzias, A. A. and Wilson R. W. *ApJ*, 142, 419-221, 1965.
5. Smoot, G. F. et al. *ApJL*, 291, L23, 1985.
6. Fixsen, D. J., Cheng, E. S., Gales, J. M., Mather, J. C., Shafer, R. A., & Wright, E. L. *ApJ*, 473, 576, 1996.
7. Zannoni, M. et al. in proceedings of the *International Conference on 3K Cosmology EC-TMR, Roma 1998*, edited by L. Maiani, F. Melchiorri and N. Vittorio, AIP Conference Proceedings 476, 1999, p. 165.
8. Bennett, C. L. et al. *ApJ*, 464, L1, 1996.
9. de Bernardis, P. et al. *Nat*, 404, 955, 2000.
10. Hanany, S. et al. *ApJ*, 545, L5, 2000.
11. Carretti, E. et al., this volume
12. Caderni, N., Fabbri, R., Melchiorri, B., Melchiorri, F., & Natale, V. *PhysRevD*, 17, 1901, 1978.
13. Nanos, G. P. *ApJ*, 232, 341, 1979.
14. Lubin, P. M. & Smoot, G. F. *ApJ*, 245, 1, 1981.
15. Partridge, R. B., Nowakowski, J., & Martin, H. M. *Nat*, 331, 146, 1988.
16. Wollack, E. J., Jarosik, N. C., Netterfield, C. B., Page, L. A., & Wilkinson, D. *ApJ*, 419, L49, 1993.
17. Netterfield, C. B., Jarosik, N., Page, L., Wilkinson, D., & Wollack, E. *ApJ*, 445, L69, 1995.
18. Sironi, G. et al., *NewA*, 3, 1, 1998.
19. Subrahmanyan, R., Kesteven, M. J., Ekers, R. D., Sinclair, M., & Silk, J. *MNRAS*, 315, 808, 2000.
20. Hedman, M. M., Barkats, D., Gundersen, J. O., Staggs, S. T., & Winstein, B. *ApJL*, 548, L111, 2001.
21. Keating, B. G., O'Dell, C. W., de Oliveira-Costa, A., Klawikowski, S., Stebor, N., Piccirillo, L., Tegmark, M., & Timbie, P. T. *ApJL*, 560, L1, 2001.
22. Carretti, E., Tascone, R., Cortiglioni, S., Monari, J., Orsini, M., *NewA* 6, 173–187, 2001.
23. Jonas, J. L., Baart, E. E., Nicolson, G. D. *MNRAS*, 297, 977, 1998.
24. Hauser, M. G., et al, *ApJ*, 508, 25, 1998.
25. Tegmark, M., Eisenstein, D. J., Hu, W., & de Oliveira-Costa, A., *ApJ*, 530, 133, 2000.
26. Reich, P. & Reich, W., *A&AS* 63, 205
27. Boen, K. this volume.
28. Baldemar, P., Widell, O. this volume.
29. Sbarra, C. et al. this volume.
30. Delabrouille, J. *A&AS*, 127, 555, 1998.
31. Wright E. L., *astro-ph*/9612006.
32. Carretti E., et al., 2001 in preparation.
33. Revenu, B., Kim, A., Ansari, R., Couchot, F., Delabrouille, J., & Kaplan, J. *A&AS*, 142, 499, 2000.
34. Tascone R. et al. *AIP 2K1BC Conference Proceeding, Cervinia (Ao), 2001 in press.*
35. Macculi C. et al. *AIP 2K1BC Conference Proceeding, Cervinia (Ao), 2001 in press*.
36. Macculi, C. & Zannoni, M. this volume.
37. J. R. White, Origin and Measurement of Internal Stress in Plastics, Polymer Testing, 4, 165–191, 1984.
38. E. D. Palik, Handbook of optical constants of solid II, Academic Press, 1991.
39. Macculi C., Spurious polarisation from dielectrics, *BaR-SPOrt Int. Tech. memo*, 2000.